Decay of quasi-bounded classical Hamiltonian systems populated by scattering experiments

1995 J. Phys. A: Math. Gen. 28 4235

(http://iopscience.iop.org/0305-4470/28/15/004)

J. Phys. A: Math. Gen. 28 (1995) 4235–4243. Printed in the UK

Decay of quasi-bounded classical Hamiltonian systems populated by scattering experiments

A J Fendrik† and M J Sánchez‡
Departamento de Física, Facultad de Ciencias Exactas y Naturales, Universidad de Buenos Aires, Ciudad Universitaria, 1428, Buenos Aires, Argentina

Received 1 July 1994, in final form 15 February 1995

Abstract. We study numerically the decay of a Hamiltonian system whose transient bounded dynamics is fully chaotic but not necessarily fully hyperbolic when the phase space is initially populated by scattering experiments. We show that parabolic subsets included in the trapped orbits set are related to an algebraic tail corresponding to long times. The characteristic exponent of such a tail and that corresponding to the tail of the decay from the equilibrium population differ by one. This fact, already observed in other non-hyperbolic systems, is related to internal distributions that characterize the internal dynamics of the system.

1. Introduction

A survey of decay events and scattering processes in complex systems gives valuable information about them. As remarked in a recent work [1] both experiments are closely related. Thus in the case of Hamiltonian systems the properties that reveal themselves in temporal decay laws and time delay distributions are determined by the characteristics of the invariant sets of trapped orbits.

In this work we study the scattering events on a potential related to Sinai's billiard (it is alo called Sinai's well) model [2]. We consider independent point particles of unit mass in the two-dimensional potential $V(x, y)$:

$$V(x,y) = \begin{cases} \infty & \text{if } x^2+y^2 \leqslant R^2 \\ -V_0 & \text{if } |x| < a/2,\ |y| < a/2 \text{ and } x^2+y^2 > R^2 \\ 0 & \text{if } a/2 \leqslant |x| \text{ or } a/2 \leqslant |y| \end{cases}$$

where x, y are Cartesian coordinates and $R < a/2$. Let us remark that unlike other extensively studied non-integrable billiard systems, where the connection between the external and internal regions is provided by holes in rigid boundaries [3, 4], in the present system the total energy E is a relevant parameter. In this sense, our system can be related to those in [5], where the circular billiard with a hole in the boundary which can be permeable according to the total energy of the particle is studied. We will consider here particles with fixed E such that $0 < E$. Thus, the particles have the total energy to cover all the plane. However, particles inside the well stay there, their Cartesian components v_i, $i = x, y$ of the velocity $\boldsymbol{v}$ are such that

$$\frac{|v_i|}{|\boldsymbol{v}|} \geqslant \frac{1}{\sqrt{1+V_0/E}} = \sin\psi_{\text{lim}} \tag{1.1}$$

† Member of CONICET.
‡ Fellowship CONICET.

0305-4470/95/154235+09$19.50

when they reach the square boundary. We call this motion quasi-bounded.

In the following we will fix a (the side of the square-well) as a unit of length. Provided $m = 1$, $a/\sqrt{2(E+V_0)}$ has units of time, hence we can take it as a unit of time such that the only dependence on the total energy E is condition (1.1). Thus, without loss of generality we can take $|v| = 1$ inside the well. In this way elapsed time and length of the corresponding trajectory on the configuration space are equivalent.

In previous works [6, 7] we have studied the decay of Sinai's well from the microcanonical population (in the following equilibrium population) and we have related the decay law to internal distributions that characterize the well's internal dynamics. The invariant set of trapped orbits of the present problem is fully hyperbolic, or it includes non-hyperbolic subsets (parabolic) according to the value of R, the radius of the central scatterer. In [6] we show that the fully hyperbolic character of the invariant trapped orbits is related to a purely exponential decay law while the existence of parabolic trapped orbits leads to a crossover between exponential decay and an algebraic decay. It is evident, from relation (1.1), that dynamics with $E > V_0$ leads to $\psi_{\lim} > \pi/4$ so, in such a case, there are no trapped parabolic periodic orbits (periodic orbits that miss the central scatterer and fulfil condition (1.1)) no matter what the value of R. For this reason we will consider particles with fixed E such that $0 < E < V_0$.

In this work we are interested in the global consequences on the population temporal laws for scattering experiments when parabolic subsets are included in the trapped set.

2. The time delay

The existence of non-hyperbolic subsets makes itself evident in the typical observables for scattering events such as the deflection function or the time delay as a function of the impact parameter ρ for a given (fixed) incident angle γ_i [8, 9].

The scattering processes can be understood as follows. When the incident projectile hits the central scatterer (first collision) its velocity could be re-orientated in such a way that condition (1.1) holds. In this case the particle remains in the well, rebounding with the square boundary and the central scatterer until a final bounce with the central scatterer could re-orientate the velocity such that condition (1.1) is not fulfilled and the particle leaves the well. Between the first and final collision the motion is quasi-bounded. We can distinguish two cases. The first corresponds to $R > R_c = \sqrt{2}/4$ and all the trapped orbits involve at least one additional collision with the central scatterer, that is they are hyperbolic. The internal dynamics are dominated by collisions with the central scatterer so we have fully hyperbolic irregular scattering. In this case the number of internal reflections on the square boundary between two collisions with the central scatterer cannot exceed three, so the time delay increases according to the number of collisions with central scatterer n. Figure 1(a) shows a representative orbit. In such a case we will observe the characteristic behaviour in the time-delay function related to the non-integer fractal dimension of the trapped set [10]. Figure 2(a) shows this hyperbolic time delay for $R = 0.38$ and $\gamma = \pi/4$. We could see the self-similarity mentioned above by expanding the horizontal scale (ρ) to improve resolution. In this case the values of the ordinate (T) corresponding to similar regular segments (the flat lines) increase with the number of hits n, as we have previously remarked.

The second case corresponds to $R < R_c$ and where there is a subset of parabolic trapped periodic orbits that miss the central scatterer included in the invariant trapped set (they involve only internal reflections on the square boundary). As a consequence, for some intervals of impact parameter ρ between two collisions with the central scatterer there could be internal motion dominated by reflections on the square boundary. Figure 1(b)

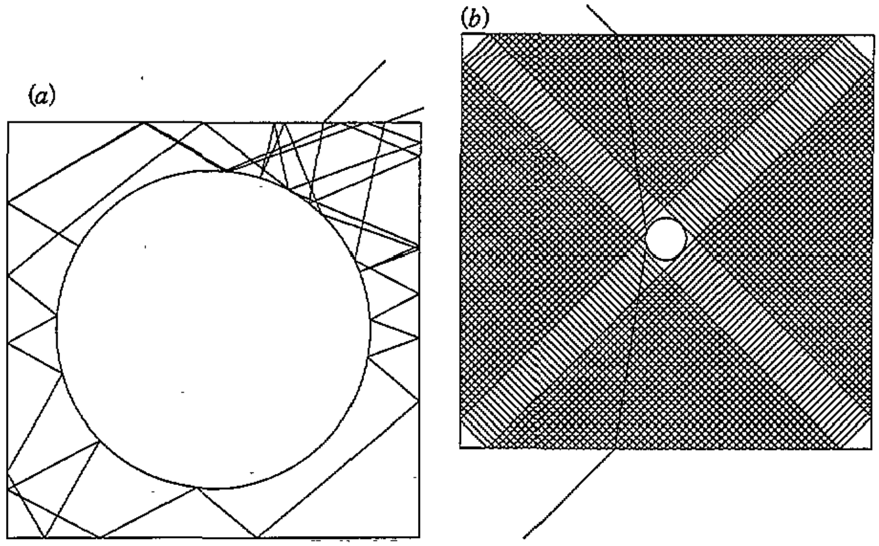

Figure 1. Two orbits of scattering experiments. (*a*) $R > R_c$. The set of periodic trapped orbits is fully hyperbolic. The internal motion is sketched by collisions with the central scatterer. (*b*) $R < R_c$. The set of periodic trapped orbits includes parabolic subsets. There can be internal motion characterized by reflections in the square boundary.

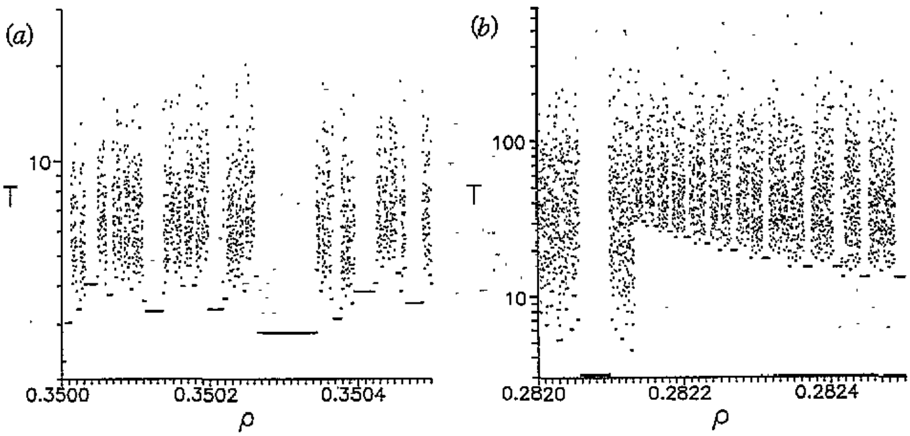

Figure 2. Log–linear plot of time delay τ against impact parameter ρ corresponding to a trapped set: (*a*) fully hyperbolic; (*b*) including parabolic subsets.

shows a representative orbit. Therefore, the time delay function increases according to the number of internal reflections on the square boundary between two collisions with the central scatterer, in addition to the number of collisions with the central scatterer n. This fact originates a regular background over which the hyperbolic time delay is mounted. Figure 2(*b*) shows this situation. The background can be analytically determined and its origin becomes clearer using the extended version of the system (square ordered Lorentz gas) [11–13] where parabolic orbits correspond to channels between the scatterering centres (see appendix A).

3. The decay

As already pointed out in [1], the decay and the scattering events for a fully chaotic system (that is a system that does not have regular islands) differ in the initial population of the phase space. The first problem assumes that the system is fully bounded at the beginning (i.e. the well behaves like a billiard, in the present problem the Sinai billiard, such that the particles are fully confined at the beginning) and the decay starts from the statistically stationary population (microcanonical) when particles are allowed to escape [6]. In the scattering experiments, the initial population of the phase space depends on the characteristic of the incident beam. This beam leads to a well-localized population in the phase space, generally in a subset whose dimension is smaller than the dimension of the energy shell. Therefore, we can modify the formalism of [6] to relate the scattering decay law to the internal dynamics and we can test some results obtained from the study of the decay in [6] by employing them in the scattering calculations.

We summarize the results derived in [6] that allow us to relate the decay from the equilibrium population to the internal dynamics:

$$\hat{Q}(s) = \frac{w\hat{g}_e(s)/s}{1-(1-w)\hat{f}_e(s)} \tag{3.1}$$

where $\hat{Q}(s) = \mathcal{L}[Q(t)]$ means the Laplace transform and

$$Q(t) = 1 - N(t)/N_0. \tag{3.2}$$

Here $N(t)/N_0$ is the fraction of particles present in the well at time t (that is the decay law) and (see [6])

$$w = \frac{1}{\pi} 4 \arcsin \frac{1}{\sqrt{1+V_0/E}} \tag{3.3}$$

is the probability that one particle leaves the well after one bounce with the central scatterer. To obtain (3.1), we crudely assume that the velocity autocorrelation goes to zero after one collision with the central scatterer. The distributions $g_e(t)\,dt$ and $f_e(t)\,dt$ are the fraction of particles whose first collision with the central scatterer occurs between t and $t+dt$ and the fraction of particles whose time between two successive collisions with the central scatterer is between t and $t+dt$ respectively. $g_e(t)$ and $f_e(t)$ correspond to equilibrium (in the sense that was pointed out at the beginning of the present section) and they are related by the condition

$$\frac{dg_e}{dt} = -g_e(0) f_e(t) \tag{3.4}$$

which was proved in [6]. Moreover, in [6] it was shown that $g_e(t)$ with finite horizon, that is its decreasing is exponential or faster, leads to an exponential decay of the remaining population $N(t)/N_0$. Otherwise (algebraic decreasing) the decay shows a crossover from exponential to algebraic behaviour for long times.

As we have already said, for this work (scattering events) $g(t)$ is arbitrary, depending on the particular incident beam, we call it $g_p(t)$ and condition (3.4) does not hold. Here we will consider a uniform parallel beam of point particles whose incoming velocity subtends a fixed angle γ_i with the normal direction corresponding to one side of the square well (see figure 3). We will only consider the incident particles that bounce with the central scatterer because if they miss it, they leave the well by the opposite side. Such a beam corresponds

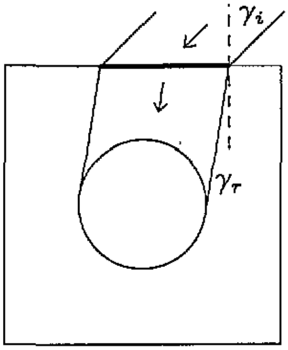

Figure 3. Sinai's well potential, the beam (arrows), the region uniformly populated (thick line) by the beam and angles $\gamma_{\rm i}, \gamma_{\rm r}$.

to a uniform population of particles on a segment of length $2R/\cos\gamma_{\rm r}$ on the side of the square well whose velocity subtends an angle

$$\gamma_{\rm r} = \arcsin\frac{\sin\gamma_{\rm i}}{\sqrt{1+V_0/E}}. \qquad (3.5)$$

The resulting distribution $g_{\rm p}(t)$ is like a pulse centred in $\tau_0 = (1/(2\cos\gamma_{\rm r}) - \pi R/4)$ and width $R(1+\tan\gamma_{\rm r})$. For the sake of simplicity, we ignore the details of $g_{\rm p}$ keeping only the relevant features (namely the finite horizon and the temporal localization) and taking

$$g_{\rm p}(t) \approx \delta(t-\tau_0). \qquad (3.6)$$

Alternatively, as the collisions with the central scatterer are the mechanism used to reach equilibrium we assume, as in [6] for the derivation of relation (3.1), that after a collision the velocity autocorrelation function goes to zero, that is statistical loss of memory on the initial population occurs so that the distribution $f(t)$ must correspond to the equilibrium $f_{\rm e}(t)$. This assumption will be strongly justified by our final results. Therefore, the modified version of relation (3.1) is

$$\hat{Q}_{\rm p}(s) = \frac{w\hat{g}_{\rm p}(s)/s}{1-(1-w)\hat{f}_{\rm e}(s)}. \qquad (3.7)$$

In the following we calculate the rate

$$\frac{N(t)}{N_0} = 1 - Q_{\rm p}(t) \qquad (3.8)$$

where $Q_{\rm p}(t) = \mathcal{L}^{-1}[\hat{Q}_{\rm p}(s)]$, using (3.7) for the scattering on a potential whose trapped set includes only one parabolic subset related to the non-isolated parabolic periodic orbits characterized by $|v_x|/|v_y| = 1$. That is $\sqrt{5}/10 < R < \sqrt{2}/4$. In this case we know that (see [6])

$$f_{\rm e}(t) = C\left([\delta(t) - \delta(t-T_0)] + \Delta(R)\sum_{j=2}^{\infty}(1/j)^2\{\delta[t-(j-1)T_0] - \delta(t-jT_0)\}\right). \qquad (3.9)$$

In expression (3.9)

$$\Delta(R) \equiv \alpha\left(1 - \frac{R}{\sqrt{2}/4}\right)^{\beta} \qquad (3.10)$$

with $\beta = 1.4776$ and $\alpha = 0.2741$,

$$(T_0)^{-1} = \frac{2R}{(1-\pi R^2)} \tag{3.11}$$

and

$$C = \frac{1}{T_0[1+\Delta(R)(\zeta(2)-1)]} \tag{3.12}$$

with $\zeta(2) \equiv \sum_{n=1}^{n=\infty} 1/n^2$.

The resulting $\hat{Q}_{\mathrm{p}}(s)$ is

$$\hat{Q}_{\mathrm{p}}(s) = \frac{w}{s}\frac{\exp(-\tau_0 s)}{w-(1-w)[1-\exp(sT_0)][\exp(-sT_0)+\Delta(R)\sum_{n=2}^{n=\infty}\exp(-nsT_0)/n^2]} \tag{3.13}$$

which depends on R (through τ_0, T_0 and $\Delta(R)$), E (through w) and γ_{i} (through τ_0). The latter dependence appears as a temporal translation that is irrelevant for $t \gg \tau_0$. We stress that expression (3.13) is quite determined, that is, it does not have free parameters because we use those that were established in [6] for the decay.

We calculate the rate $N(t)/N_0$ for $R = 0.23$, energy $E = V_0/20$ and $\gamma_{\mathrm{i}} = \pi/4$ by numerical simulation and by inverse transformation of (3.13). For the numerical simulation calculation we consider 10^7 particles initially uniformly distributed on a segment of length $2R/\cos\gamma_{\mathrm{r}}$ belonging to one side (see figure 3) whose unity velocity subtends an angle γ_{r} with the normal to the side given by (3.5). Figures 4(*a*) and (*b*) shows the results. There we can observe a satisfactory fit between both calculations. At first there is an exponential decay relating the population of asymptotic conditions to the hyperbolic trapped subset (see figure 4(*b*)). Later there is a power behaviour relating the population of asymptotic conditions to the parabolic subset. Such algebraic behaviour for the tail corresponding to long times is $\sim 1/t^{\alpha_s}$ with $\alpha_s = 2$. Thus taking account the fact that the tail for the decay problem from the equilibrium population is $\sim 1/t$ (see [6]), we conclude

$$\alpha_s - \alpha_t = 1 \tag{3.14}$$

as according to [1].

Actually, relation (3.14) can be seen as a consequence of (3.4) together with (3.1) and (3.7). For the decay from the equilibrium, the leading term of (3.1) gives

$$Q(t) \sim w\int_{t'=0}^{t'=t} g_{\mathrm{e}}(t')\,\mathrm{d}t' = w\left(\int_{t'=0}^{t'=\infty} g_{\mathrm{e}}(t')\,\mathrm{d}t' - \int_{t'=t}^{t'=\infty} g_{\mathrm{e}}(t')\,\mathrm{d}t'\right). \tag{3.15}$$

As was shown in [6], for long times t, $g_{\mathrm{e}}(t) \sim 1/t^2$, so $Q(t) \propto (1-1/t)$ and $N(t)/N_0 \propto 1/t$. Alternatively, for the decay from the population by scattering experiments, the leading term of (3.7), taking into account (3.4), results in

$$\begin{aligned} Q_{\mathrm{p}}(t) &\sim w(1-w)\int_{t'=\tau_0}^{t'=t} f_{\mathrm{e}}(t'-\tau_0)\,\mathrm{d}t' \\ &= w(1-w)\left(\int_{t'=\tau_0}^{t'=\infty} f_{\mathrm{e}}(t'-\tau_0)\,\mathrm{d}t' - \int_{t'=t}^{t'=\infty} f_{\mathrm{e}}(t'-\tau_0)\,\mathrm{d}t'\right) \end{aligned} \tag{3.16}$$

where $f_{\mathrm{e}}(t) \sim 1/t^3$ for long times. Therefore, $Q(t) \propto (1-1/t^2)$, $N(t)/N_0 \propto 1/t^2$ and (3.14) holds. The difference between the exponents given by (3.14) was also observed and explained in [5] for the case of a system whose internal dynamics is purely regular.

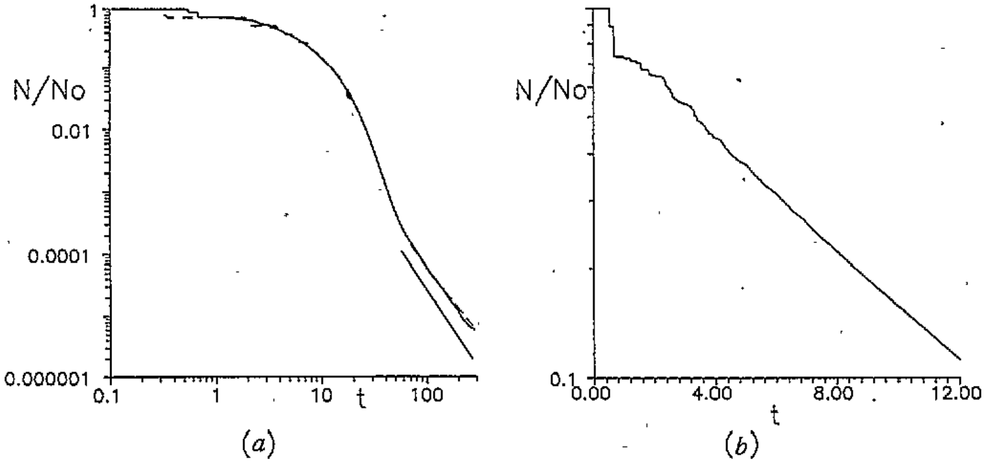

Figure 4. (*a*) Log–log plot of the remaining population inside the well $N(t)/N_0$ against t. The broken curve corresponds to that calculated using (3.13) while the full curve corresponds to the exact calculation. We have also drawn the straight line of slope two to clarify the characteristic exponent of the algebraic long-time tail of the decay law. (*b*) Log–linear plot of $N(t)/N_0$ against t to display the exponential behaviour for short times in the actual decay law.

4. Summary and conclusions

We have shown how a parabolic subset of trapped orbits modifies the time delay pattern in an irregular scattering process. The parabolic subset provides a regular background over which the hyperbolic pattern is seen.

We have also established that the existence of a parabolic subset leads to an algebraic decay law for long times $\sim 1/t^2$ when the system is populated by scattering experiments. The characteristic exponent differs by one from that corresponding to decay from the equilibrium population.

As we have mentioned before, to derive expressions (3.1) and (3.7) we assume that the loss of memory in the direction of velocities occurs after one collision with the central scatterer. This fact and the results displayed in figure 4 suggest that the main difference between the decay from the equilibrium population and the decay from the population by scattering is that the first is dominated by the loss of memory in the direction of velocities from the equilibrium distribution. This loss of memory is related to the distribution $g_e(t)$ that gives the fraction of particles whose first collision with the central scatterer occurs between t and $t + \mathrm{d}t$. The decay process in the scattering experiment is dominated by the distribution $f_e(t)$, that is, following (3.4), the temporal rate of the memory loss.

To finish, we remark that the equilibrium distributions $g_e(t)$ with finite horizon (i.e. exponentially decreasing or faster) in (3.1) lead to an exponential decay from the equilibrium population as was shown in [6]. According to relation (3.4) the corresponding distributions $f_e(t)$ will have a finite horizon, so, following (3.7), the decay from the population by our beam will also be exponential when $R > \sqrt{2}/4$.

Appendix A.

This appendix is devoted to explaining the regular background of the time delay function when there are parabolic trapped orbits. Let us consider that the projectile has an impact parameter ρ such that after colliding with the central scatterer its internal dynamics is non-hyperbolic until the final collision, as figure 1(a) shows. Because the internal velocity is constant, the time delay will be the length L of the internal trajectory. To evaluate this as a function of the impact parameter it is convenient to use an extended version of Sinai's well, namely the square ordered Lorentz gas. The length L will be determined by the ratio between the width of the channel δ and the shift in the direction of the velocity with respect to the direction of the channel after the first bounce . Here we will determine L for the channel that corresponds to parabolic orbits characterized by the ratio $v_y/v_x = \pm 1$, which has directions $\pm\pi/4$ and $\delta = (\sqrt{2}/2 - 2R)$.

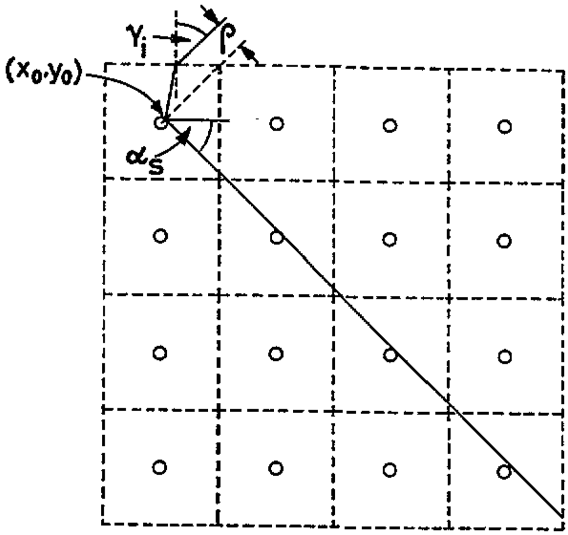

Figure A1. Scattering experiments in the extended version of Sinai's well. γ_i is the incidence angle, ρ is the impact parameter, (x_0, y_0) is the point of the hit with the central scatterer, α_s is the angle between the velocity after the hit and the x axis.

Firstly, we determine the point (x_0, y_0) where the projectile hits the central scatterer as a function of the impact parameter ρ and the angle γ_i (see figure A1):

$$x_0 = \frac{\sqrt{(m^2+1)R^2 - b^2} - mb}{1+m^2} \qquad y_0 = mx_0 - b \tag{A.1}$$

where

$$m = \frac{v_y}{v_x} = \cot\gamma_r = \frac{\sqrt{(V_0/E) + \cos^2\gamma_i}}{\sin\gamma_i} \tag{A.2}$$

$$b = \frac{1}{2} - m\left(\frac{1}{2} - \frac{\rho - 1/2(\cos\gamma_i - \sin\gamma_i)}{\sin\gamma_i}\right). \tag{A.3}$$

We then evaluate the α_s, corresponding to the direction of the velocity after the bounce:

$$\tan\alpha_s = \frac{|-2x_0y_0 - (y_0^2 - x_0^2)m|}{|(y_0^2 - x_0^2) - 2x_0y_0m|}. \tag{A.4}$$

To finish, we find the shift of α_s with respect to the direction of the channel; in the present case $(\pi/4 - \alpha_s)$. For projectiles in the channels, this angle is much smaller than one,

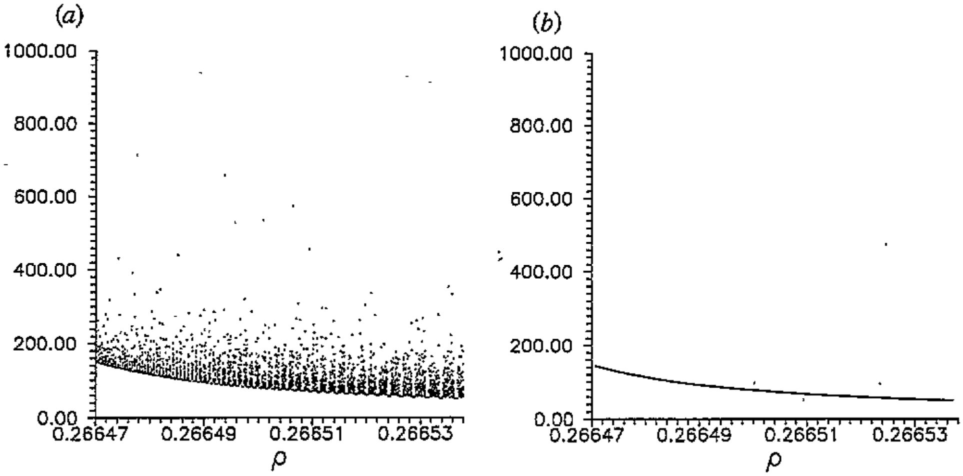

Figure A2. (a) A piece of the time-delay function corresponding to a region of the impact parameters such that the internal motion is dominated by the parabolic subset of trapped orbits $v_y/v_x = 1$. (b) The regular background predicted by (A.6) (see the text) for $R = 0.05$, $\gamma_1 = \pi/4$ and $V_0/E = 20$.

therefore

$$(\pi/4 - \alpha_s) \approx \tan(\pi/4 - \alpha_s) = \frac{1 - \tan\alpha_s}{1 + \tan\alpha_s} \tag{A.5}$$

thus,

$$L(\rho) \approx \frac{(\sqrt{2}/2 - 2R)(1 + \tan\alpha_s(\rho))}{1 - \tan\alpha_s(\rho)}. \tag{A.6}$$

Figure A2(a) shows a part of the actual time delay function corresponding to a region of the impact parameters such that the internal motion is dominated by the parabolic subset of trapped orbits $v_y/v_x = 1$. Figure A2(b) shows the regular background predicted by (A.6) for $R = 0.05$, $\gamma_1 = \pi/4$ and $V_0/E = 20$.

References

[1] Pikovsky A S 1992 *J. Phys. A: Math. Gen.* **25** L477
[2] Sinai Ya G 1970 *Russ. Math. Surveys* **25** 137
[3] Bauer W and Bertsh G F 1990 *Phys. Rev. Lett.* **65** 2213
[4] Jensen R V 1991 *Chaos* **1** 101
[5] Dumont R S and Brumer P 1989 *J. Chem. Phys.* **90** 96
[6] Fendrik A J, Rivas A M F and Sánchez M J 1994 *Phys. Rev.* E **50** 1948
[7] Fendrik A J and Sánchez M J 1995 Decay of the Sinai well in *D* dimensions *Phys. Rev.* E **51** 2996
[8] Ott E and Tèl T 1993 *Chaos* **3** 417
[9] Gaspard P and Rice S A 1989 *J. Chem. Phys.* **90** 2225
[10] Smilansky U 1991 *The Classical and Quantum Theory of Chaotic Scattering (Les Houches LII)* ed M J Giannoni, A Voros and J Zinn-Justin (Amsterdam: North-Holland)
[11] Zacherl A, Geisel T, Nierwetberg J and Radons G 1986 *Phys. Lett.* **114A** 317
[12] Bouchaud J P and Le Doussal P 1985 *J. Stat. Phys.* **41** 225
[13] Friedman B and Martin R F Jr 1984 *Phys. Lett.* **105A** 23